



Development of an Ultra-Stable Mid-Infrared Detector Array for Space-Based Exoplanet Transit Spectroscopy

*Technology Milestone White Paper
Proposal # 18-SAT18-0024*

Johannes G. Staguhn^{1,2} (PI),
Dale Fixsen², Kevin Stevenson³, Elmer Sharp², Ari Brown², Jonathan Fortney⁴, Gene Hilton⁵,
Tiffany Kataria⁶, Karwan Rostem², Edward Wollack², Avi Mandell²

¹Johns Hopkins University ²NASA Goddard Space Flight Center, ³STScI,
⁴UC Santa Cruz, ⁵NIST-Boulder, ⁶JPL

May 27, 2020



Approvals:

Released by

Johannes Staguhn
Principal Investigator

Date

Approved by

Brendan Crill
Exoplanet Exploration Deputy Program Chief Technologist, JPL

Date

Nick Siegler
Exoplanet Exploration Program Chief Technologist, JPL

Date

Douglas Hudgins
Exoplanet Exploration Program Scientist, NASA HQ

Date



Table of Contents

1.0	OBJECTIVE	1-1
2.0	INTRODUCTION	2-1
2.1	RELEVANCE FOR FUTURE EXOPLANET MISSIONS.....	2-2
2.2	SENSITIVITY, DYNAMIC RANGE	2-3
2.3	MID-IR SPECTROMETER TECHNOLOGIES.....	2-4
2.3.1	<i>Detectors</i>	2-4
2.3.1.1	Impurity Band Conduction Detectors (IBC).....	2-4
2.3.1.2	Superconducting Photon Counters	2-5
2.3.1.3	Transition Edge Sensors (TES)	2-5
2.3.2	<i>TES for MIR Spectroscopy</i>	2-6
2.3.3	<i>Need for a calibration system</i>	2-7
2.3.4	<i>Laboratory Demonstation</i>	2-7
3.0	SPECTROMETER OPTICS AND OPERATION	3-9
3.1	DIFFERENCES BETWEEN FLIGHT AND LABORATORY DEMONSTRATIONS	3-10
4.0	MILESTONES AND SUCCESS CRITERIA	4-10
4.1	MEASUREMENT OF THE EXO-PLANET	4-10
4.2	MILESTONE DEMONSTRATION PROCEDURE	4-10
4.2.1	<i>Data analysis</i>	4-12
4.3	SUCCESS CRITERIA: STABILITY ACHIEVED FOR THESE MEASURMENTS WILL	4-13
5.0	CERTIFICATION	5-13
5.1	MILESTONE CERTIFICATION DATA PACKAGE.....	5-13
6.0	REFERENCES AND CITATIONS.....	6-14

1.0 Objective

This whitepaper describes the purpose and context of this proposal for NASA's Exoplanet Exploration Program (ExEP) within the NASA Strategic Astrophysics Technology (SAT) program. The stated goal is the *Development of an Ultra-Stable Mid-Infrared Spectrometer for Space-Based Exoplanet Transit Spectroscopy*. We describe the methodology for assessing the Technology Development for ExEP-SAT milestone metrics, and establish the success criteria against which the milestone will be evaluated. The main milestone is the demonstration of an ultrastable spectrometer we call *MIRASET* (Mid-IR Array Spectrometer demonstration for Exoplanet Transits) that will allow the extraction of mid-infrared spectral lines observed in the atmospheres of transiting planets around M-stars that potentially indicate the presence of life on the planet. As reference, transits of the habitable zones (HZ) planets around TRAPPIST-1 have a duration of ~ 2 hours. The required sensitivity for such measurements is 5 parts per million (ppm), which has not been demonstrated, nor is expected to be achievable with currently existing MIR spectrometers such as MIRI on JWST. Demonstration of a spectrometer with this precision and stability presents the required success criterion for having achieved the stated goal of the proposal. A more comprehensive discussion of the general spectrometer idea can be found in Staguhn et al., 2019a.

2.0 Introduction

One of the primary goals of the astrobiology community in particular, and the broader astrophysical and planetary science communities in general, is the ability to detect the presence of biosignatures on habitable worlds. Habitability is typically defined as the ability of a planet to sustain liquid water on its surface. It is primarily a function of incident radiation, but can also depend on other factors such as UV flux, atmospheric composition, etc. Spectroscopic characterization of terrestrial atmospheres will provide constraints for climate models to assess the potential for habitability.

In the mid-infrared, the main observable is a planet's dayside emission spectrum, as measured using the secondary eclipse technique. For terrestrial exoplanets orbiting within the HZ of mid-to-late M-dwarf stars, the planet-to-star flux contrast ratio becomes favorable at wavelengths $> 5 \mu\text{m}$ (see Figure 1). Accounting for the decrease in photon count rate at longer wavelengths, the signal-to-noise ratio is favorable out to $\sim 25 \mu\text{m}$. Within this wavelength range, there are prominent absorption features due to CH_4 , CO_2 , O_3 , NH_3 , N_2O , and SO_2 , as well as the H_2O vapor continuum. These features can readily distinguish a wet Earth-like planet from a dry, Venus-like planet with a dense CO_2 atmosphere and a Mars-like planet with a thin CO_2 atmosphere (see Figure 1). The strong ozone band at $9.7 \mu\text{m}$ allows for detecting the presence of molecular oxygen in the atmosphere, which is a powerful biosignature when combined with other out-of-equilibrium molecular species (such as CH_4 at $7.7 \mu\text{m}$ and/or N_2O at $17 \mu\text{m}$). Additionally, emission spectroscopy uniquely probes a planet's thermal structure, which is critical towards assessing its habitability. The required sensitivity for the observation of a spectral line in transit observations is given by

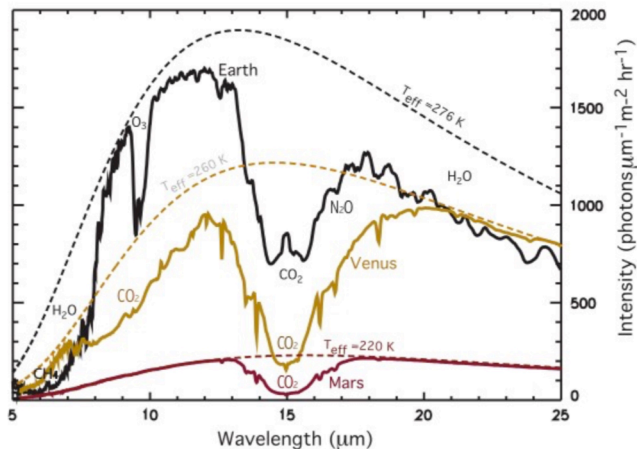


Figure 1. Relative intensity of planetary emission as a function wavelength for three terrestrial planet models. Bands for ozone, carbon dioxide, nitrous oxide, and water vapor can all be readily observed at $> 8 \mu\text{m}$. Depending on the planet-star contrast ratio, methane may or may not be detectable in emission at $7.7 \mu\text{m}$. However, methane can still be detected in transmission.

The strong ozone band at $9.7 \mu\text{m}$ allows for detecting the presence of molecular oxygen in the atmosphere, which is a powerful biosignature when combined with other out-of-equilibrium molecular species (such as CH_4 at $7.7 \mu\text{m}$ and/or N_2O at $17 \mu\text{m}$). Additionally, emission spectroscopy uniquely probes a planet's thermal structure, which is critical towards assessing its habitability. The required sensitivity for the observation of a spectral line in transit observations is given by

the ratio between the line depth and the "continuum" emission from the stellar host. This required ratio is independent of the telescope size, but it only depends on the type of planet and its host star. The simultaneous detection of the biosignatures O_3 and CH_4 or O_3 and N_2O requires a sensitivity of 5 ppm in the measurement, and with the fact that transit observations last a few hours, requires an ultrastable spectrometer to be achievable.

Milestone definition:

Laboratory Demonstration of a Mid-IR spectrometer with a two-hour stability, required to observe transits of HZ planets around Trappist-1, to enable the detection of biosignatures in the atmospheres of transiting planets around M-stars.

Using a black body source simulating the M-star's emission, we will demonstrate the ability to monitor over a 2-hour period a laser-generated spectral line down to a precision of 5ppm or better on top of this black body emission source which dissipates the equivalent power on the detectors that would be observed from Proxima Cen and Trappist-1 if they were observed with a space based telescope such as ORIGINS.

2.1 RELEVANCE FOR FUTURE EXOPLANET MISSIONS

In preparation for the *New Worlds, New Horizons* (NWNH) decadal survey four Great Observatory Studies are being executed at this time. One of those is the *Far Infrared Surveyor* (now the

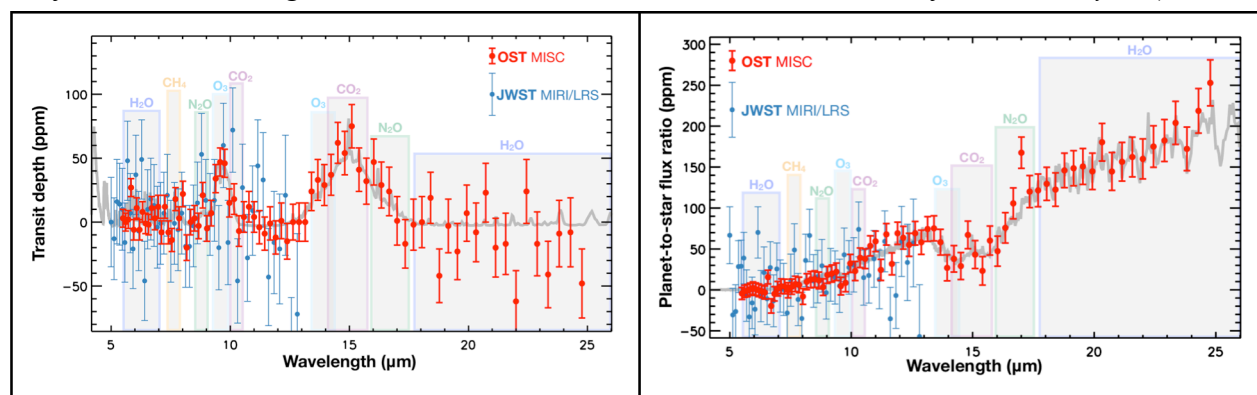


Figure 2. OST’s MISC transit spectrometer channel, using an ultrastable spectrometer as proposed here, will characterize habitable planets in search of signs of life. Model transmission (A) and emission (B) spectra of TRAPPIST-1e (0.92 R_E , 250 K), but at a closer distance of 4.2 parsec with simulated data shows OST’s improvement in precision and wavelength coverage over JWST. The following spectroscopic lines are present in the band shown here: (H_2O , CO_2) and bio-signatures (O_3 , CH_4). These lines are interesting biosignatures.

Origins Space Telescope, "Origins" study, which includes 5 instruments, one of which is a mid-IR camera with integrated Transit Spectrometer for the detection of bio-signatures in exoplanets in the habitable zone around M-dwarfs (Figure 2). The aim of this proposal is to provide a mid-IR spectrometer with integrated calibration system that will enable this capability, which current mid-IR detectors cannot achieve. Future dedicated Explorer- or Probe-studies for dedicated MIR Transit Spectroscopy missions will also benefit from this demonstration of an ultrastable MIR spectrometer (see e.g. Staguhn et al., 2019b).

2.2 SENSITIVITY, DYNAMIC RANGE

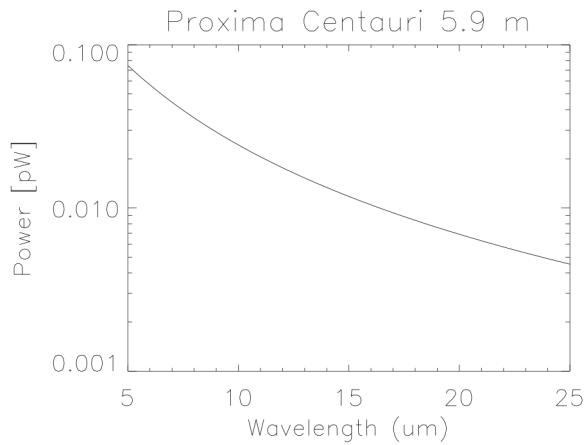


Figure 3a) Expected Photon Load from Proxima Centauri, observed with a 5.9 m diameter telescope with an optical efficiency of 50% The solid line is the expected power per detector element behind a spectrometer with a spectral resolution of $R \sim 100$ across the 5-25 μm band.

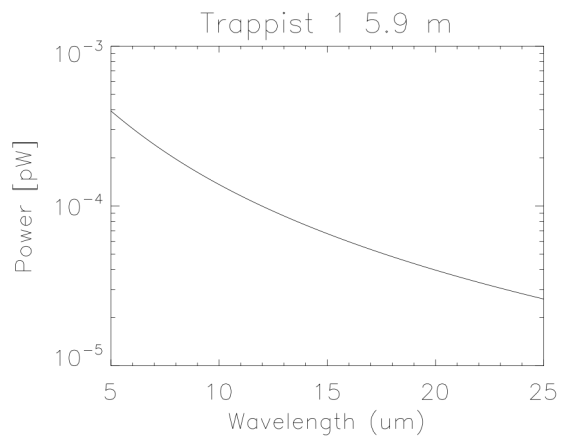


Figure 3b) Expected Photon Load from Trappist-1, observed with a 5.9 m diameter telescope with an optical efficiency of 50% The solid line is the expected power per detector element behind a spectrometer with a spectral resolution of $R \sim 100$ across the 5-25 μm band.

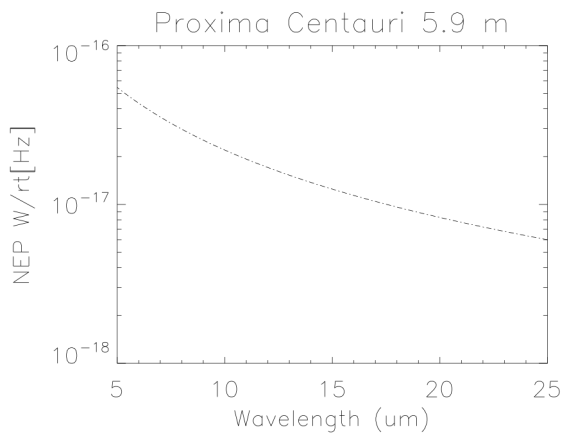


Figure 3c) Expected Photon Noise from Proxima Centauri, observed with a 5.9 m diameter telescope with an optical efficiency of 50% The solid line is the expected power per detector element behind a spectrometer with a spectral resolution of $R \sim 100$ across the 5-25 μm band.

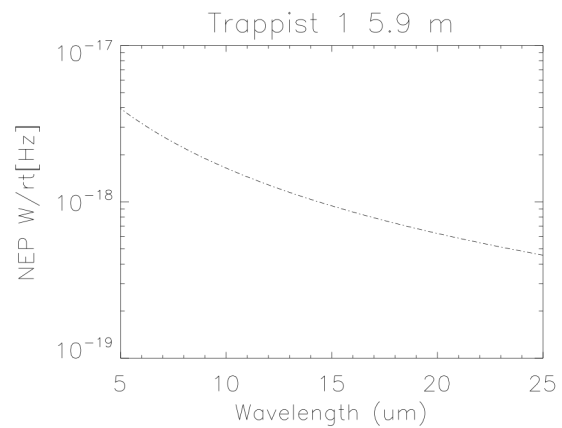


Figure 3d). Expected Photon Noise from Trappist-1, observed with a 5.9 m diameter telescope with an optical efficiency of 50% The solid line is the expected power per detector element behind a spectrometer with a spectral resolution of $R \sim 100$ across the 5-25 μm band.

The aim of a mid-IR Transit Spectrometer is to study the atmospheres of exoplanets, particularly those in the habitable zone. Here we explicitly assume an Origins sized mirror of 5.9 m, looking at the phase curve of a planet orbiting around Proxima Centauri as proxy for the most luminous source, and as the other extreme observations of planets in the Trappist system. Note that the actual science requirement for Origins is to observe a TRAPPIST-1e-like planet with an Earth-like atmospheric composition, orbiting a closer Trappist-1 type (i.e. M8) star with $K_{\text{mag}}=9.85$, which corresponds to a distance of 10 pc (rather than 12 pc for the actual Trappist-1 star).

Proxima Centauri is a M dwarf with a temperature of $\sim 3,040$ K with a diameter of $2 \cdot 10^8$ m at a distance of $4 \cdot 10^{16}$ m. It will radiate ~ 820 pW into a 25 m^2 mirror near earth. An earth-sized planet at the distance of Proxima will radiate about $4 \cdot 10^{-8}$ of that or about $3.3 \cdot 10^{-5}$ pW.

By restricting the observations to 5-25 μm , one can take advantage of the relatively higher emission of the planet in this range, which has 24,000 fW of star light but still .26 fW from the planet. Assuming a telescope efficiency of 50% and a dispersion resulting in an average spectral resolution $R = \nu / \Delta\nu \sim 100$ puts 4 to 65 fW per bin on the detector from the 25 μm to the 5 μm end of the band (the exact wavelength dependent power per spectral channel is shown in Fig. 3). The comparable numbers for the planet are $4 \cdot 10^{-5}$ to $6 \cdot 10^{-4}$ fW. Thus we can calculate the total number of photons at each wavelength from the star and from the planet.

The photons are Poisson distributed so the photon noise from the star is just the square root of the number of photons. Although the planet can be observed for longer than the transit time, ultimately the noise will be limited by the time that the star can be observed without planet. The observations can be repeated at each transit. This shows that in principal the detailed emission from the exoplanet can be observed with a very stable high efficiency detector.

Instrument Key Attributes:

- Photon-noise limited performance
- High stability
- Sufficient dynamic range for Transit Spectroscopy
- Integrated high-precision calibration

We show the numbers for our extreme examples Proxima Centauri and Trappist-1 in Fig. 3 a, b for the observed power, and Figs. 3c and 3d for the observed Noise Equivalent Bandwidth of the star's photons. Over a mission lifetime of a few years tens of planetary systems could be studied in the range defined by these examples.

In the following section (2.3) we show that existing Transition Edge Sensors can meet both the loading and sensitivity requirements.

2.3 MID-IR SPECTROMETER TECHNOLOGIES

2.3.1 DETECTORS

2.3.1.1 IMPURITY BAND CONDUCTION DETECTORS (IBC)

Spitzer IRAC Si:As detectors have demonstrated about 60 ppm precision in transit observations of several hours. JWST/MIRI is expected to achieve similar or slightly better stability (Bright, et al., 2016). Limiting factors in stability are currently not sufficiently understood. After the launch of JWST in 2021, MIRI is expected to show some improvement of the state-of-the-art for stability beyond that achieved by Spitzer/IRAC (Greene et al., 2016). In particular, additional work in on-orbit calibration of transit spectroscopy observations will show how much instability can be corrected in the presence of drifts in the instrument and in the astrophysical sources. The intrinsic stability of the mid-IR detector system may be driven by fundamental detector materials properties, cryogenic detector readout circuitry (which is not optimized for operation at cryogenic temperatures), or other instabilities in the system. For future missions such as Origins, which require a detector stability of a few parts per million over hours, a detailed study of instabilities in MIR detectors will be needed to determine where technology investments will be most effective. This should be done in concert with modeling in-orbit calibration, which will mitigate the detector requirements to some level. Additionally, alternative dopings for IBC detectors (such as phosphorous) need to be considered as a less costly alternative to arsenic doping for mid-IR detectors. *However, with all the uncertainties in the achievable performance of IBC detectors, it is prudent to look into alternative detector technologies.*

2.3.1.2 SUPERCONDUCTING PHOTON COUNTERS

The number of photons/second per spectrometer pixel for Proxima Centauri, a proxy for the brightest M-star potentially being targeted with *MIRASET* on a 5.9 m telescope (Origins) is ~ 5 million per spectral channel at the short wavelength side of the observed spectrum. Therefore, only very fast photo counting detectors could be used. Photon counters based on MKIDs e.g. are too slow.

Other than photo-counting MKIDs or the Quantum Capacitance Devices, Superconducting Nano-wires can be read out at tens of MHz rates and therefore are a potential candidate. The problem is that those devices have not been demonstrated at mid-IR wavelengths, but are currently being used at shorter wavelengths, (shortward of $2 \mu\text{m}$; the technology as such has not been demonstrated at $> 7 \text{ mm}$). As the wavelength increases, there are likely to be a number of issues that will become relevant, two of which are: as the energy per photon goes down, the biasable range necessary to obtain the required high detection efficiency in the nanowire gets smaller and the contribution of dark currents to the readout precision rises. Furthermore, basic physics suggests one needs to reduce the width of the wire to $< 20 \text{ nm}$ almost and order of magnitude below the 150 nm demonstrated. This is only ~ 50 atoms and film uniformity variations will play a major factor in the performance of the devices. Multiplexers for the readout of larger arrays are still in development.

2.3.1.3 TRANSITION EDGE SENSORS (TES)

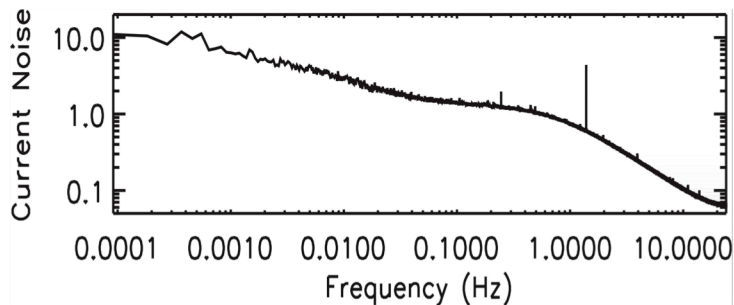


Figure 4. Long duration laboratory measurement of the average noise spectrum of a Goddard TES Detector array (in units of normalized current noise density).

mode feature (since each SQUID multiplexer reads out several detectors). TES are also less prone to vibrational or electromagnetic pickup than higher-impedance KIDs and semiconducting devices, which more often show resonant features in their noise spectra. The Physics of TES is well understood in detail, so the performance of those devices can be reliably designed.

Fig. 4 shows the averaged measurement of 667 pixels of one of our TES arrays in the laboratory, with common mode subtracted. The detectors are low-pass filtered with a one-pole filter, so the slope at high frequencies shows this $1/f$ attenuation of the signal. The full signal between 1 Hz and several tens of second is almost flat, while at times greater than ~ 1 minute there is a slight upturn in the noise. However, the slope is moderate. We would like to note that the ADR (Adiabatic Demagnetization Refrigerator) was not in feedback mode during the measurements and so the increase in noise longwards of $\sim 20 \text{ mHz}$ is mostly due to temperature fluctuations, typical for systems like this. While this detector will be perfectly suitable for \sim minutes and shorter integration, in order to maintain stability on timescales of minutes to several hours a calibration system will be needed in order to maintain the requirements of *MIRASET*.

2.3.1.3.1 GISMO: DEMONSTRATED SUCCESS OF TES DETECTOR TECHNOLOGY

Since fielding of the instrument in 2007, GISMO has been operated at the IRAM 30-m telescope in Spain for many years. The instrument was made available to the general astronomical community. Observations with GISMO have yielded ground-breaking scientific data on high-redshift

galaxies, including observations of a high-redshift submillimeter galaxies published in two separate articles in the journal *Nature* (Capak et al., 2011; Riechers et al., 2013). The main reason for GISMO's success is the significant stability of the instrument.

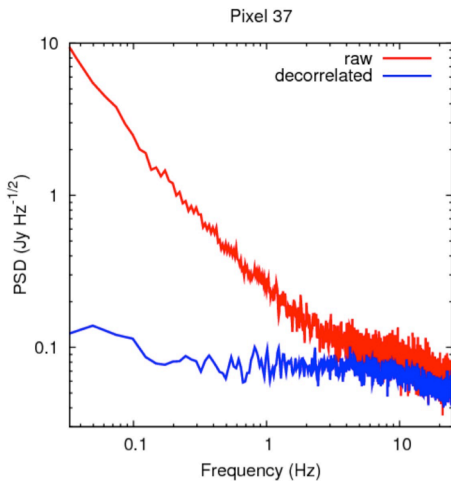


Figure 5. Noise spectra of GISMO detectors on the sky: *Red*: Averaged noise of individual pixels showing the sky variations as $1/f$ noise. *Blue*: Common mode subtracted average pixel noise shows no residual $1/f$ down to well below 0.1 Hz.

detector gains and offsets remain constant over the entire observing time of the area on the sky covered by the emission, which in case of the Galactic Center Observations shown in Figure 6 corresponds to several minutes of observing time.

2.3.2 TES FOR MIR SPECTROSCOPY

We have developed very stable, large format, high efficiency low noise TES-Transition Edge Sensor (TES) based bolometer arrays operating from the mid-infrared to submillimeter, wavelength regimes (Benford et al., 2010). These arrays have been successfully integrated into the GISMO bolometer camera and the SOFIA 2nd generation instrument HAWC+; more will follow to be integrated into GISMO-2, and PIPER. All detectors for these instruments were produced at NASA/GSFC. Most of the collaborators on this proposal had strong involvement in these projects. The PIPER and HIRMES detectors have sufficient sensitivity and dynamic range for mid-IR spectroscopic applications, such as *MIRASET* which requires detectors with noise equivalent power (NEP) of $\sim 10^{-18}$ W/ $\sqrt{\text{Hz}}$ and a saturation power of less than 0.1 pW for its core science case between 5 μm and 17 μm , where the main biosignature lines can be found. For planet temperature measurements at longer wavelengths at lower spectral resolution, the HIRMES detectors also meet the sensitivity requirements. (For even higher requirements on the detector noise, there are more sensitive TES detectors available that have been demonstrated e.g. at SRON, with NEP of $\sim 10^{-19}$ W/ $\sqrt{\text{Hz}}$, Suzuki et al., 2015).

Since TES are used as bolometers (the resistance changes with temperature) they can be used at any wavelength, as long as the incoming radiation can be coupled efficiently into the detector membrane. Therefore, and in order to save funding, we propose to use an *existing* TES array from the HIRMES project (HIRMES uses absorbers that operate in the MIR), which meets the sensitivity and dynamic range requirements for a space based mid-IR transit spectrometer for Origins. The required detectors absorption can be tuned, so that a high quantum efficiency can be achieved. However, for simplicity of our proposed experiment, we will not incorporate quarter wave resonators into the detector arrays for this demonstration.

Figure 5 demonstrates the stability of the detectors during the observations: while the $1/f$ noise of the sky variations can be seen as a strong signal in individual

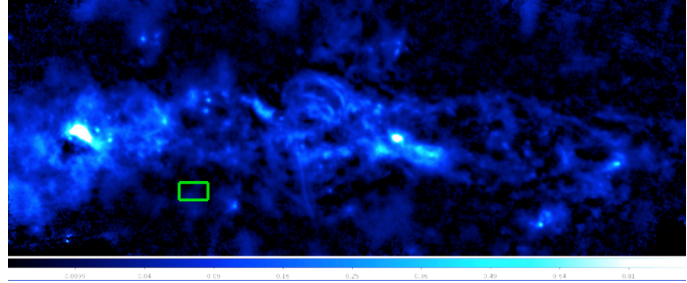


Figure 6. The GISMO 2 mm Galactic Center map (observed in a total of 6.5 hours) shows extended emission in angular scale well in excess of the GISMO detector size (green box).

pixels (red), these variations can be completely removed to well below 0.1 Hz by subtracting the common mode in all pixels (blue; note that most of the sky variations happen in the near-field where all pixel beams do completely overlap). Extended emission exceeding the array size can only be recovered, if the

2.3.3 NEED FOR A CALIBRATION SYSTEM

A calibration system will be necessary, since there are no known infrared detectors that provide 5 ppm stability over many hours (Greene et al., 2016). The calibration scheme for *MIRASET* is independent of the detector used (the detector needs only provide a sufficient signal to noise ratio for calibrating individual time intervals of ~ 100 s, so the detector just needs to be stable within that shorter time frame. Stability of TES over 100s has been demonstrated (section 1.3.2.2). Should better detectors become available in the future, the calibration scheme we describe here could be used to improve the long-term stability of those, too.

The proposed effort will be an important demonstration of a new mid-IR detector and calibration technology, necessary to enable the detection of bio-signatures in planetary atmospheres with The Origins Space Telescope (OST). The required spectrometer stability over many hours, needed for the detection of bio-signatures in the atmospheres of exo-planets through transit spectroscopy in the mid-IR will only be possible through a very stable detector array plus an integrated ultra-stable calibration scheme as proposed here. We emphasize that the stability requirement for the detector is significantly more relaxed than the requirement for the spectrometer and it is independent of the distance to the observed planet.

2.3.4 LABORATORY DEMONSTATION

To provide an adequate demonstration, both the spectral resolution and the stability of *MIRASET* over several hours need to be demonstrated. A prototype instrument (schematic shown in Figure 7, design drawing in Fig. 8) will be built in a modified lab cryostat to maintain the detectors and the rest of the instrument at stable temperature. The optical input will be simulated with an external integrating sphere with intervening filters and a mask (or masks). Stability is the key for the simulation. A simple tungsten filament operating at 2000-2500K is sufficient to generate a spectrum over the 5-25 μm range of the instrument. With a 1 mm^2 element the total evaporation rate is of the order of 1 atom per sec allowing a very long life and potentially stable operation. A 1 mm^2 surface emits ~ 1 W blackbody radiation. Since only of order 1 pW is required for the detector, significant filtering and baffling can be used to put only a small fraction of the total light on the detector. The monitor and the filament will be in a vacuum at 4K. The feedback electronics will be adjusted to account for the thermal and electrical time constants of the filament and its current driver.

A stable mechanical configuration will be required, so the entire mechanical 4 K assembly will be temperature controlled. We have already obtained the required PID controller and have demonstrated its capability to keep the 100 mK detector stage in our lab dewar at a constant temperature within only 1.5 μK rms over many hours. The same PID electronics will be used to control the 4K stage, the laser at 50K, and the warm readout electronics at stable temperatures with using heaters at all these stages. We will also control the tungsten filament optical output: To monitor the black body temperature at high precision, we will utilize a (photo-diode) sensor at ~ 500 nm, which we already have purchased. Since 500 nm is on the Wien side of the black body peak, a small change in temperature results in a large change in emission. For a 2200 K blackbody the change at 500 nm is 7 times the change at 5 μm and 11 times the change at 25 μm . Thus measuring the changes at 500 nm to one part in 20,000 will allow stabilization of the BB (tungsten filament) to 5 ppm, the knowledge of its temperature at any time will likely be even more accurate. This requirement will be easily met with a photo diode: We are planning to use the Vishay BPW21R. As expected the dark current drops with temperature and at the temperature we will be using it, the dark current will not be an issue. The specification of the Vishay BPW21R says the change with respect to temperature is .05%/K so in order to get 5e-6 we only need to maintain the temperature of the diode to .01 K, and due to the higher gain of 7 at 0.5 μm

for temperature measurements, roughly 0.1 K temperature fluctuations will be within the range of requirements. We have already demonstrated this in the existing dewar. One note of caution here, we are using the Vishay BPW21R outside of its normal temperature range. However, we have already verified that it works at 4K, but need to demonstrate that its performance stays within specifications at that temperature.

MIRASET will also demonstrate the required resolution and frequency stability over several hours. A laser at 6 μm will be used to verify this. The most critical measurements can be made overnight. This allows hours of stable operation with minimal disturbance from neighboring laboratories.

The overall plan is to test the various subsystems first and then integrate them into the overall system. The major subsystems are the cryostat and its temperature readout system, the light source and its stabilization electronics, and the TES and its readout SQUIDs and electronics. The major requirement for the cryostat is to keep its contents at a cold (4K) stable temperature, which will be obtained by the active temperature control of the stage. The TES must be cooled to ~ 100 mK for proper operation, the active temperature control of both these stages will provide the required stability in the optical coupling of sphere and detector. The range of bias currents of the TES detector will be explored to find optimum settings to maximize stability and sensitivity. The readout will use the same clock as the electronics for the thermometers and the source feed back to minimize clock noise and phase wander.

Once the subsystems are tuned up and working, a single night of data acquisition, say from 9 PM to 7 AM, will be enough to show the system sensitivity and stability. A weak signal from the laser will show that we can recover a small signal during an hour-long integration. Although a single night is sufficient, undoubtedly we will repeat for several nights to verify the results are reproducible. One operation that will be explored is flipping back and forth between two levels of emission with a period of a few minutes to check the system for gain stability.

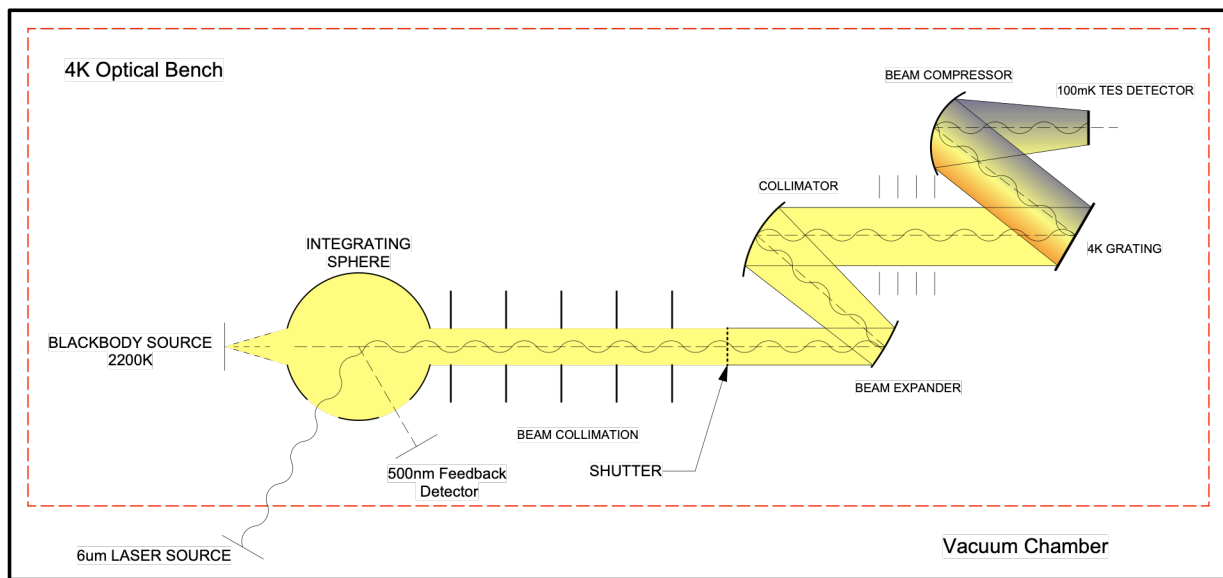


Figure 7. Schematic showing the proposed experiment. The calibration system (blackbody source, integrating sphere, and the photo-diode for temperature monitoring) are all at 4 K together with the cold optics, mid-IR grating, and the TES detector array at 100 mK. The infrared laser will be temperature controlled at the 50 K stage. Note that the optical coupling of the laser will not be very sensitive to temperature fluctuations and that the laser only serves as frequency calibration. Amplitude variations in the laser output will not affect the accuracy of the calibration.

3.0 Spectrometer Optics and Operation

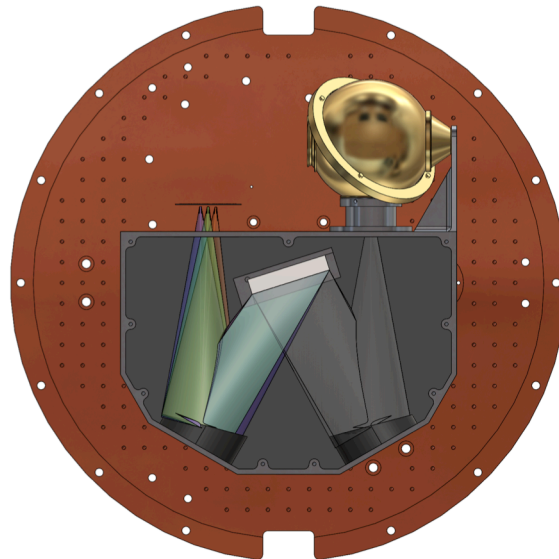


Figure 8. Top view of the MIRASET Spectrometer: The light, which is a combination of the emission from the Tungsten wire and the MIR laser, is mixed in the integrating sphere. It illuminates a ~ 1 mm slit wide at the focus of an off axis parabolic mirror. The mirror then relays the light to a diffraction grating (GR2550-07106) with 75 lines/mm. The grating then reflects the light to a second parabolic mirror with its focus on the detector. The detector is a TES detector with ~ 1 mm pixels. At this distance the dispersion is such that each pixel covers $\sim .1 \mu\text{m}$ so the resolution will be 60-70 over the range of our limited detector.

MIRASET is only a test to demonstrate the principle rather than an optimized model of the final instrument. The optical layout is straightforward. The light, which is a combination of the attenuated emission from the Tungsten wire and the MIR laser light illuminates a slit ~ 1 mm wide at the focus of an off axis parabolic mirror. The mirror then relays the light to a diffraction grating (GR2550-07106) with 75 lines/mm. (We recognize that the grating is too fine, but it is readily accessible and funds are limited.) The grating then reflects the light to a second parabolic mirror with its focus on the detector. The detector is a TES detector with ~ 1 mm pixels. At this distance the focused beam of is approximately 1 pixel wide. The dispersion is such that each pixel is $\sim .1 \mu\text{m}$ so the resolution will be 60-70 over the range of our limited detector. We might also change the position and grating to look at the long wavelength end. In a real instrument we would need a second diffraction to separate different orders in the cross dispersion direction.

All of the parts from the slit to the TES detector are in an aluminum box painted on the inside with Z306 to make it black. It will also be cooled to 4 K to minimize emission from the walls. The temperature of the BB radiation from the tungsten filament will be modulated on a \sim minute timescale between two states, e.g. 2200 K and 2100 K to create the "A/C coupling" that allows for the calibration. The attenuation of the BB radiation is such that its photon noise is less than the noise from every star that will be observed with the space instrument, therefore allowing for

the detectors to observe the astronomical signal simultaneously with the BB radiation from the filament.

3.1 DIFFERENCES BETWEEN FLIGHT AND LABORATORY DEMONSTRATIONS

The optical configuration in the lab is obviously different, since the BB radiation and the "source signal" (laser) get combined in the instrument's sphere, whereas in space the source (star plus planet) enters through the primary while we intend to mix it with the BB radiation at the position of the secondary mirror of the telescope. This will ensure that both share most of the optical train in the observatory.

At L2 the flight environment will be more stable than the laboratory environment. First at L2 there is no diurnal cycle making the thermal environment much more stable. There is no vibration except those introduced by the spacecraft itself meaning the mechanical environment is much more stable. Finally L2 is far away from cell phones and other radiofrequency electrical interference.

4.0 Milestones and Success Criteria

4.1 MEASUREMENT OF THE EXO-PLANET

The scientific product provided by the spectrometer will be the measurement of the planet's transmission and/or emission spectrum. The measured spectrum is dominated by the BB emission from the star. Superimposed on this BB radiation will be the spectral features due to the planet's atmospheric lines, which can be in emission or absorption. Examples include CO, O₃, H₂O, and others. This "small signal" from the planet is on top of the star's significantly stronger emission and will need to be cleanly separated. The stated goal for the precision of this measurement is 5 parts per million (ppm).

4.2 MILESTONE DEMONSTRATION PROCEDURE

The requirement is 5 ppm stability in the instrument measurement capability. The stability will be mostly affected by: 1. Stability of photo diode. 2. Stability of the MIR laser. 3. Instrument's temperature stability. 4. Detector stability. 5. Black body source (BB) stability. 6. Optical stability, which is dominated by the mechanical robustness of the instrument. *However, we emphasize apart from the photo diode (and for this experiment the laser) that these components need to be stable only between two measurements of the black body temperature of the radiation from the 100 filament, since this measurement allows a total recalibration of the spectrometer's gain and offset!* The BB temperature measurement can be done to the required sensitivity of 5 ppm for the MIR spectral region within 100 seconds or less, because the measurement itself is being obtained in the visible by the photo diode, where only $5 \times 7 = 35$ ppm precision is required to obtain the needed signal to noise ratio. During 100 s integration time, however, the requirement for stability of the detectors is significantly lower, simply due to the noise properties of the observed targets, the two most extreme of which are shown in Figure 3. For Proxima Centauri the signal to noise ratio implies only a required stability of $\sim 10^{-3}$ within a second (Figures 3a and 3c), resulting in a stability requirement of $\sim 10^{-4}$ in 100s. For Trappist observations, the stability requirement is even down to 10^{-3} in 100 seconds. As has been shown for a low noise TES, the dynamic range of a TES would not even allow a 5 ppm observation within a second (Staguhn 2018). The active temperature control of the various components plus of the BB source is primarily done to mini-

mize short-term variations (< 100 s) and second order effects, such as change of the spectral shape of the BB SED.

The following table contains the main instrument components:

Part	requirement
Photo diode	35ppm -> temperature stabilization better than 0.1K
Detector	100ppm (100 seconds) -> $\Delta T < 10\mu\text{K}$
Tungsten filament	100 ppm (100 seconds) -> $\Delta T < 0.2$ K
Grating	5ppm freq. stabil. -> mechanically stable to 0.25 arcsec
MIR laser	5ppm -> tbd

The following milestones will be achieved during this project:

- a) ADR temperature stability demonstration (with and w/o feedback control)

a) We will measure the open loop temperature stability of the ADR-base temperature. A following step will use our PID control system for the ADR-base temperature and aim at regulating the ADR temperature stability to be better than $1\mu\text{K}$ rms. Base temperature fluctuations on the detector stability depend on the difference between base temperature and transition temperature of the detector, but are expected to be in the order of these fluctuations over the T_c of the detector ($\sim 10\text{mK}$), or $\sim < 10$ ppm (for a detailed analysis see Benford et al. 2004). Once the detectors have been installed and verified in the spectrometer, we will measure this conversion factor by measuring the detector response to temperature variations in the ADR base temperature. If necessary, though extremely unlikely necessary, stability requirements for the ADR control could be adjusted accordingly. As demonstrated earlier, it is by far not necessary to obtain a stability of 5 ppm for the detector over 100s, the actual requirement is 100 ppm (10^{-4}) or larger. The major source for temperature variations potentially resulting in such large variations on short time scales are coming from the cryo-cooler, which could induce temperature variations with significant amplitudes. However, we aim to show that stable frequency variations in the base temperature can be suppressed by a factor of 100 or better, and we anticipate that those variations will average out to a significant degree over the many hour measurements. We would also like to note that in space applications, the cryo-coolers are commonly driven by linear motors. We are exploring whether we can afford such a linear drive motor for our lab cryo-cooler.

Description of Measurement: We will monitor the open loop ADR temperature fluctuations for the duration of an ADR cycle (over night measurement), while at the same time monitoring ambient temperature in the lab. We will then take 5 1-hour measurements of the ADR temperature with open loop, adjusting the PID parameters for each run. The number of iterations can be increased, if optimal performance has not been obtained (better than $11\mu\text{K}$ rms). Having found the optimal PID loop parameters, we will repeat the measurement with closed loop for another night. We will reduce the data and look at FFT and verify that we have achieved the stability goal defined above.

- b) Measurement of the Black Body (BB) temperature stability with and without feedback control

In this step we measure the BB stability with the photo-diode with and without PID control. We will verify that the required sensitivity of the measurement will be achieved in the predicted amount of integration time to verify our prediction for the achievable signal to noise (s/n) ratio (in ~ 100 seconds).

We will show that we can stabilize the temperature of the filament to within 0.5%

at 2200 K. We will also show that we can switch between a couple of filament temperatures e.g. 2100 and 2200 K reliably within a minute or less. These measurements will be repeated 3 times.

- c) Measurement of spectrometer frequency stability through monitoring of laser spectral lines

This milestone requires the complete integration of the MIR detectors into the spectrometer. We will perform a measurement of the spectral lines of our MIR laser source. The goal of this test is to quantify the frequency stability of the spectrometer. This is an important metric, since any variations in the spectrometer that result in frequency changes effectively reduce the ability to detect atmospheric lines. Even a small shift results in an apparent gain change because the stellar spectrum rises steeply in this regime. We will measure the frequency stability vs temperature of the laser in order to derive the requirement needed to obtain 5 ppm, and attempt to determine if any instability is due to the instrument or the laser itself.

- Measurement of BB curve and spectral stability thereof

Once the frequency stability of the laser has been quantified we will determine the "broader" frequency stability by fitting the correct BB SED to the measured BB temperature. This will be done by repeatedly switching between two temperatures of the BB (knowledge of the absolute temperatures for both states are not needed). We will obtain the following 4 measurements: Overnight observation of 5 different black body temperatures: one with the filament heated to a temperature that produces a power of 0.01 pW on the detector array with ORIGINS which corresponds to the power from Proxima Cen during a real mission (Figure 3a), one with 0.0001 pW, corresponding to the emission from Trappist-1 observed with ORIGINS and two measurements (Figure 3b) with the BB at 2,100 and 2,200 K. We will repeat each measurement 3 times to demonstrate repeatability.

- Verification of overall stability in measurement over days

The final instrument characterization will be a combination of all measurements described above, taken over the duration of several days in order to quantify the long-term stability of the system. When the system is run over several successive nights, we will measure the stability of the instrument and the reproducibility of the gain and offset from one night to the next to a few ppm. These measurements will be done obtained for the extreme cases of optimal tungsten attenuation fan temperature settings for Trappist and for Proxima Cen (Figures 3a and 3b). These observations will be repeated 3 times to demonstrate repeatability.

4.2.1 DATA ANALYSIS

Data is collected from each channel as well as from thermometers inside and outside the dewar. Operation of MIRASET is highly automated. After setup and initial adjustment, the instrument will be operated over weekends when the traffic in the laboratory is very low. These observing runs will generate long data sets. We will take advantage of the fact that these detectors and the data collection system is almost time stationary. For stationary systems the Fourier transform generates data in the frequency domain where the different frequencies are independent. In frequency domain, the cryocooler frequencies and ADR instabilities, usually appear at sharp frequencies (and their harmonics). Thus it is easy to associate sources with the resulting noise in the TES data. But we can also perform a linear correction. The reduction in noise is an indication of the importance of the particular noise sources, but it also shows how much improvement can be expected in post observation corrections to the TES data. Since there are a large number of pixels (128 and 512, respectively for the two detectors we currently have available) we will also be able to remove common mode instability using principle component analysis.

The fit coefficients connecting the optical detector and the TES detector is a direct data this can be determined to a few parts per million. By looking at this coupling for several light source settings the absolute temperature of the tungsten filament can be determined.

The long integration times will also allow analysis at very low frequencies, to 100 μHz . This illuminates the prospects of operating for longer than a few hours for an eclipse perhaps into the time frames of phase observations of planets orbiting close to their parent stars. The repeatability of the measurements can be examined by looking at 3 weekends.

The data analysis can be used to help determine noise sources. These can then be attacked physically by stabilizing the offending source, and by using measurements on the source to fit and remove the noise. The two methods are not mutually exclusive, and linear regression can simultaneously mitigate multiple sources of noise as well as suggest which ones need to be treated in the physical instrument.

4.3 SUCCESS CRITERIA: STABILITY ACHIEVED FOR THESE MEASUREMENTS WILL

Success criteria for our lab spectrometer performance are straightforward: demonstration of the **calibrated** spectrometer stability to 5 ppm over 2 hours and more*, which is required for the Trappist-1 HZ planets. If we can show that this stability can be obtained over the entire band, we do not need to do a more sophisticated analysis of the data. However, even if there are still residual common-mode gain- and offset variations in the data, demonstration of successful removal of those, still obtaining a spectral accuracy, which can be demonstrated on the laser spectral lines in the lab setup will be required. Obviously, the very challenging stability requirement will only be demonstrable, if the laser itself is stable to within those limits. Fortunately, with the BB temperature control, we will not need to re-calibrate the spectral response of the detectors and therefore with the help of our calibration system will be able to quantify the spectral stability of the laser.

* Once we have obtained a continuous ADR from a separate SAT project at Goddard, we will be able to demonstrate many hours to a day of stability, not a requirement for Transit spectroscopy of HZ planets around M-stars, but an enabler for phase curve observations. Note, however that this is not a success requirement for this SAT project.

5.0 Certification

The PI will assemble a milestone certification data package for review by the ExEPTAC and the ExEP program. In the event of a consensus determination that the success criteria have been met, the project will submit the findings of the review board, together with the certification data package, to NASA HQ for official certification of milestone compliance. In the event of a disagreement between the ExEP project and the ExEPTAC, NASA HQ will determine whether to accept the data package and certify compliance or request additional work.

5.1 MILESTONE CERTIFICATION DATA PACKAGE

The milestone certification data package will contain the following explanations, charts, and data products.

5.1.1. A narrative report, including a discussion of how each element of the milestone was met, and a narrative summary of the overall milestone achievement.

5.1.2. Data taken, which include the time stream of detector data and the following auxiliary data:

- time stream of detector data
- readout photo diode
- base temperature photo diode
- ambient temperature
- first and second stage cryo-cooler
- house keeping box
- ADR base plate
- spectrometer shell
- grating temperature
- detector package
- tungsten filament base
- laser base
- error signal on the control of the light bulb
- current on ADR
- phase of the cryocoolers

5.1.3. Reduced data products:

- raw data with common mode subtracted
- FFT of all data (incl.aux data)
- regressive fit for all aux data
- identify and remove remaining lines
- fit residual for white noise, 1/f noise, and roll off filter

5.1.4. A description of the data reduction algorithms, in sufficient detail to guide an independent analysis of the delivered data.

5.1.5. Interpretation of data, metrics met analysis.

6.0 References and Citations

Benford et al., 2004, SPIE Vol. 5498

Benford, D.J., et al., 2010, SPIE, 7741, 77411

Capak, P.L. et al., 2011, Nature 470, 233

Greene, T., et al., 2016, The ApJ, 817,17

Riechers et al., 2013, Nature, 496, 239

Rieke, G., et al., 2015, PASP, 127, 665

Staguhn, J.G., et al., 2019a, IEEE Aerospace Conference,

DOI: 10.1109/AERO.2019.8741666

Staguhn, J., et al., 2019b, Astro2020: Decadal Survey on Astronomy and Astrophysics, APC white papers, no. 238, arXiv:1908.02356

Staguhn, J.G, 2018, JLTP, 193, 908S

Suzuki, T., et al. 2015, Journal of Low Temperature Physics, DOI:10.1007/s10909-015-1401-z